



Cite this: DOI: 10.1039/c6dt00826g

Reductive nitrosylation of nickel(II) complex by nitric oxide followed by nitrous oxide release†

Somnath Ghosh,^a Hemanta Deka,^a Yuvraj B. Dangat,^b Soumen Saha,^a Kuldeep Gogoi,^a Kumar Vanka^b and Biplab Mondal*^a

Ni(II) complex of ligand **L** (**L** = bis(2-ethyl-4-methylimidazol-5-yl)methane) in methanol solution reacts with an equivalent amount of NO resulting in a corresponding Ni(I) complex. Adding further NO equivalent affords a Ni(I)-nitrosyl intermediate with the {NiNO}¹⁰ configuration. This nitrosyl intermediate upon subsequent reaction with additional NO results in the release of N₂O and formation of a Ni(II)-nitrito complex. Crystallographic characterization of the nitrito complex revealed a symmetric η²-O,O-nitrito bonding to the metal ion. This study demonstrates the reductive nitrosylation of a Ni(II) center followed by N₂O release in the presence of excess NO.

Received 1st March 2016,
Accepted 6th May 2016

DOI: 10.1039/c6dt00826g

www.rsc.org/dalton

Introduction

Transition metal ion induced activation of nitric oxide (NO) has attracted enormous research interest as various biological reactivities are attributed for forming nitrosyl complexes of metallo-proteins and mostly iron or copper-proteins.^{1,2} In this regard, the iron-nitrosyls have been studied extensively, both in protein and model systems.³ Ferriheme proteins are reported to undergo reduction in aqueous media in the presence of NO.^{4,5} The corresponding ferrous protein then reacts with excess nitric oxide to form a stable ferroheme nitrosyl.^{6–8}

The reduction of Cu(II) centers in cytochrome *c* oxidase and laccase to Cu(I) by nitric oxide has been known for a long time.^{9–12} In model systems, it has been exemplified by a number of Cu(II) complexes in recent years.^{13–23}

Mn(III) complex [Mn(PaPy₂Q)(OH)]ClO₄ (PaPy₂QH = *N,N*-bis(2-pyridylmethyl)amine-*N*-ethyl-2-quinoline-2-carboxamide) was found to react with excess NO to afford the nitrosyl complex [Mn(PaPy₂Q)(NO)]ClO₄ via reductive nitrosylation.²⁴ Another example demonstrated that adding NO to the acetonitrile solution of [(Mn(PaPy₃)₂(μ-O))(ClO₄)₂ (PaPy₃ = the anion of the designed ligand *N,N*-bis(2-pyridylmethyl)amine-*N*-ethyl-2-pyridine-2-carboxamide) resulted in the {Mn–NO}⁶ nitrosyl [Mn(PaPy₃)(NO)](ClO₄) via reductive nitrosylation.²⁵

Ni(II) in different ligand environments are known to undergo reduction to Ni(I) either by an electrochemical procedure or by

reducing agents.^{26–28} However, reduction of Ni(II) center by NO leading to subsequent nitrosylation to form {NiNO}¹⁰ complexes have not been explored extensively. Hayton's group reported examples of {NiNO}¹⁰ and their reactivity; however, in all the examples nickel(I)-nitrosyl complexes were utilized.^{29,30}

Herein, we report the NO reactivity of a Ni(II) complex, **1** of ligand **L** (**L** = bis(2-ethyl-4-methylimidazol-5-yl)methane). The ligand framework has been chosen as it offers structural flexibility and an accessible reduction potential for the transition metal ions due to its π-acceptor property. In methanol solution of complex **1**, addition of NO resulted in the reductive nitrosylation to yield the {NiNO}¹⁰ complex. This in the presence of excess NO released N₂O with the formation of corresponding Ni(II)-nitrito complex, **2**.

Results and discussion

The ligand, **L** was synthesized by following an earlier reported procedure.³¹ The Ni(II) complex, **1** was prepared by stirring a mixture of nickel(II) chloride hexahydrate with two equivalents of ligand, **L** in methanol. The microanalytical data of complex **1** shows good agreement with the calculated values (Experimental section). It was characterized by various spectroscopic analyses as well (Experimental section). The single crystal X-ray structure of complex **1** was determined. The crystallographic data, important bond angles and distances are listed in Tables 1–3, respectively. The ORTEP view of the complex **1** is shown in Fig. 1. The crystal structure revealed that the Ni(II) centre was coordinated by two ligand units in a distorted square planar geometry. The average Ni–N distance was found to be 1.893 Å, which is within the range of analogous reported complexes.³² The average N–Ni–N bite angle was ~90.0°.

^aDepartment of Chemistry, Indian Institute of Technology Guwahati, Assam 781039, India. E-mail: biplab@iitg.ernet.in

^bAcademy of Scientific and Innovative Research, National Chemical Laboratory, Pune 411008, Maharashtra, India

† Electronic supplementary information (ESI) available: All spectroscopic data and related DFT studies. CCDC 985705, 1456771 and 1456772. For ESI and crystallographic data in CIF or other electronic format see DOI: 10.1039/c6dt00826g

Table 1 Crystallographic data for complexes 1, 2 and 3

	1	2	3
Formulae	C ₂₆ H ₄₄ Cl ₂ N ₈ NiO ₂	C ₂₆ H ₄₄ ClN ₉ NiO ₄	C ₅₂ H ₈₂ Cl ₂ N ₁₈ Ni ₂ O ₇
Mol. wt	630.30	640.86	1259.68
Crystal system	Triclinic	Monoclinic	Monoclinic
Space group	<i>P</i> $\bar{1}$	<i>P</i> 2/ <i>c</i>	<i>P</i> 21
Temperature/K	296(2)	296(2)	296(2)
Wavelength/Å	0.71073	0.71073	0.71073
<i>a</i> /Å	10.8400(7)	9.4536(3)	9.7243(4)
<i>b</i> /Å	11.2885(10)	9.3089(3)	33.0698(17)
<i>c</i> /Å	14.2205(7)	18.4419(7)	9.7619(5)
α /°	85.293(5)	90.00	90.00
β /°	77.072(5)	91.025(2)	97.492(3)
γ /°	73.587(7)	90.00	90.00
<i>V</i> /Å ³	1626.57(19)	1622.68(10)	3112.4(3)
<i>Z</i>	2	2	2
Density/Mg m ⁻³	1.287	1.312	1.342
Abs. Coeff. /mm ⁻¹	0.796	0.725	0.753
Abs. correction	Multi-scan	Multi-scan	Multi-scan
<i>F</i> (000)	668	680	1328
Total no. of reflections	6030	2828	9833
Reflections, <i>I</i> > 2σ(<i>I</i>)	4214	2406	6257
Max. 2θ/°	25.50	25.00	25.00
Ranges (<i>h</i> , <i>k</i> , <i>l</i>)	−13 ≤ <i>h</i> ≤ 12 −13 ≤ <i>k</i> ≤ 8 −17 ≤ <i>l</i> ≤ 17	−11 ≤ <i>h</i> ≤ 10 −11 ≤ <i>k</i> ≤ 10 −21 ≤ <i>l</i> ≤ 21	−11 ≤ <i>h</i> ≤ 11 −37 ≤ <i>k</i> ≤ 39 −11 ≤ <i>l</i> ≤ 11
Complete to 2θ (%)	99.7	99.0	98.3
Refinement method	Full-matrix least-squares on <i>F</i> ²	Full-matrix least-squares on <i>F</i> ²	Full-matrix least-squares on <i>F</i> ²
Goof (<i>F</i> ²)	1.032	1.069	1.181
<i>R</i> indices [<i>I</i> > 2σ(<i>I</i>)]	0.0655	0.0599	0.0760
<i>R</i> indices (all data)	0.0929	0.0668	0.1297
Largest diff. peak/hole/e Å ⁻³	1.153/−1.075	1.050/−0.423	0.837/−1.034

Table 2 Selected bond lengths (Å) for complexes 1, 2 and 3

	1	2	3
Ni(1)–N(1)	1.895(3)	2.077(4)	2.050(1)
Ni(1)–N(3)	1.890(3)	2.079(4)	2.070(1)
Ni(1)–O(1)	—	2.214(4)	2.290(1)
O(1)–N(9)	—	1.268(5)	1.220(2)
N(1)–C(3)	1.337(5)	1.326(6)	1.360(2)
N(1)–C(6)	1.397(6)	1.392(6)	1.410(2)
N(2)–C(3)	1.351(7)	1.343(7)	1.340(2)
N(2)–C(4)	1.378(7)	1.374(7)	1.430(2)

Table 3 Selected bond angles (°) for complexes 1, 2 and 3

	1	2	3
N(1)–Ni(1)–N(3)	86.70 (1)	89.10(1)	90.90(4)
N(1)–Ni(1)–N(1A)	180.00(1)	171.30(2)	—
N(1)–Ni(1)–N(3A)	93.30(1)	96.80(2)	—
N(3)–Ni(1)–N(3A)	180.00(1)	94.20(2)	—
N(1)–Ni(1)–N(7)	—	—	98.50(4)
O(1)–Ni(1)–N(1)	—	86.20(1)	158.70(4)
O(1)–Ni(1)–N(3)	—	104.50(1)	86.60(4)
Ni(1)–O(1)–N(9)	—	95.40(4)	89.40(8)
O(1)–N(9)–O(1A)	—	112.40(5)	—

The complex **1** in dry methanol solution displayed absorption bands at λ_{\max} (ε/mol⁻¹ cm⁻¹), 636 (25) and 398 (240) nm in the UV-Visible spectrum along with other intra-ligand transitions at lower wavelengths (Fig. 2; ESI[†]). The band centred at

636 nm is assigned to the d–d transition for the Ni(II) center. The cyclic voltammogram of complex **1** was recorded in methanol using TBAP supporting electrolyte in a three electrode configuration with a saturated Ag/Ag⁺ reference, glassy carbon working and Pt auxiliary electrodes. A quasi-reversible reduction at −1.05 V was observed in the voltammogram (ESI[†]). These are attributed to the Ni(II)/Ni(I) reduction. In the same setup, the NO/NO⁺ couple appeared at 1.15 V (ESI[†]).

Adding an equivalent amount of NO in the degassed methanol solution of complex **1** at −80 °C displayed a shift in the d–d band from 636 nm to 578 nm (Fig. 2). The shift in λ_{\max} and change in intensity of the d–d band was attributed for forming the corresponding Ni(I)-complex (Scheme 1). Reduction of the Ni(II) center to Ni(I) by NO was also suggested from the X-band EPR studies. The diamagnetic Ni(II) center, upon adding an equivalent amount of NO became EPR active. The axial spectrum nature suggests the existence of Ni(I) (d⁹ configuration; g_{\parallel} , 2.2997; g_{\perp} , 2.1768) (Fig. 3).³³ The EPR spectra of electrochemically generated Ni(I) complexes have been reported earlier. For instance, Ni(I) complex of 5,5,7,12,12,14-hexamethyl-1,4,8,11-tetraazacyclotetradecane also displayed an axial EPR spectrum.^{33b} Double integration using Cu(II) sulphate, pentahydrate as a standard for d⁹ electronic configuration revealed the presence of ~80% Ni(I) (ESI[†]) in solution. On the other hand, the appearance of methyl nitrite in the GC-Mass spectrum of the reaction mixture also suggests NO⁺ ion was formed during the reaction (ESI[†]). This was found to be thermally unstable and highly sensitive

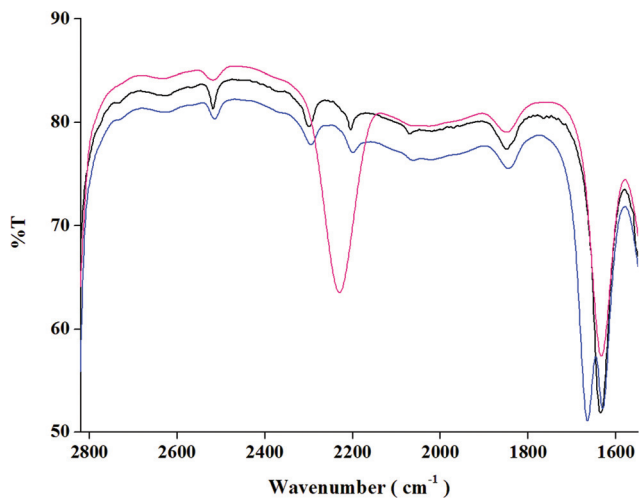


Fig. 4 FT-IR spectra of complex 1 (black), after immediate NO addition (blue); and after 30 minutes of excess NO addition (pink; N₂O formation is indicated by the peak at 2230 cm⁻¹) in methanol at room temperature.

corresponding to the {NiNO}¹⁰ intermediate. ¹⁵NO labelling shows a shift of this frequency to 1636 cm⁻¹ (ESI[†]). This frequency is actually at the low end of values reported for nickel nitrosyl complexes (ranging from 1568 to 1915 cm⁻¹).^{34,35} The nitrosyl stretching frequency was reported to appear at 1869 and 1868 cm⁻¹ in cases of [Ni(NO)(bpy)](PF₆) and [Ni(NO)(bpy)(μ-S₂Ph₂)](PF₆), respectively, in dichloromethane solution.²⁹

It is known that the geometry around the central metal ion also dictates the IR stretching frequency of metal nitrosyls. For instance, for [Ni(NO)(bpy)](PF₆), the nitrosyl stretching appears at 1869 cm⁻¹ in CH₂Cl₂, whereas at 1567 cm⁻¹ in case of [Ni(NO)(bpy)₂](PF₆); on the other hand, for [Ni(NO)(bpy)](PF₆) in acetonitrile solution, it appears at 1828 cm⁻¹ due to solvent coordination to the metal ion.³⁰ In addition, linear nitrosyls are known to have a higher stretching frequency compared to that in the bent geometry.³⁶

ESI mass spectral studies showed a peak at 584.28 suggesting formation of [Ni(L)₂(NO)(MeOH)]⁺ (Fig. 5). The isotropic distribution pattern matched very well with the simulated spectrum suggesting a correct assignment (Fig. 5). In X-band EPR studies, the {NiNO}¹⁰ intermediate appeared to be silent due to the anti-ferromagnetic coupling of spins of the paramagnetic Ni(i) and NO, resulting in an *S* = 0 spin state (Fig. 3).

In the ¹H-NMR study, the broad signals of Ni(i) species became sharp and well resolved suggesting formation of diamagnetic {NiNO}¹⁰ (Fig. 6 and ESI[†]). The proposed {NiNO}¹⁰ intermediate shown in Scheme 1 has been investigated through quantum chemical calculations employing density functional theory (DFT). The calculations were carried out using the Turbomole 6.0 suite of programs.³⁷ Geometry optimizations were performed using the Perdew, Burke, and Ernzerhof density functional (PBE).³⁸ The electronic configuration of the atoms was described by a triple-ζ basis set augmented by a polarization function (Turbomole basis set TZVP).³⁹ The resolution of identity (ri),⁴⁰ along with the multipole accelerated resolution of identity (marij) approximations were employed for an accurate and efficient treatment of the electronic Coulomb term in the density functional calculations.⁴¹ Furthermore, the solvent effects were incorporated into the COSMO model, with ε = 32.7 for methanol.⁴² The DFT optimized structure of the proposed intermediate (Scheme 1) is shown in Fig. 7 below.

As shown in Fig. 6, the {NiNO}¹⁰ intermediate has a square based pyramidal geometry with NO coordinated to nickel. It was observed that methanol does not bind to the nickel centre but remains in close proximity by forming a hydrogen bond with the nitrogen of NO, as shown in Fig. 6. The NO stretching frequency calculated with PBE/TZVP was found to be 1534.3 cm⁻¹, which was lower by 135 cm⁻¹ with respect to the experimentally observed frequency for the NO stretch. It is to be noted that the stretching frequencies obtained from DFT calculations normally differ with experiments by

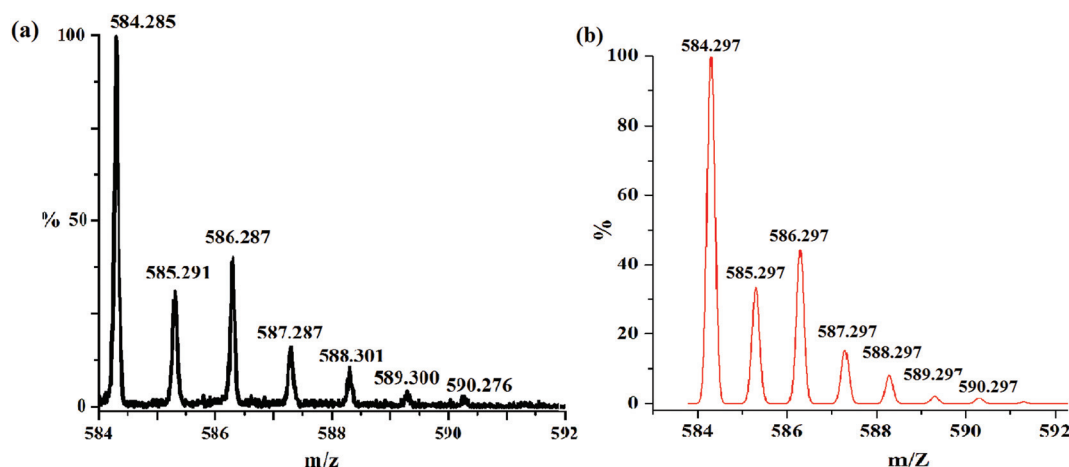


Fig. 5 ESI mass spectra of [Ni(L)₂(NO)(CH₃OH)]⁺ with isotropic distribution (a) experimental and (b) simulated.

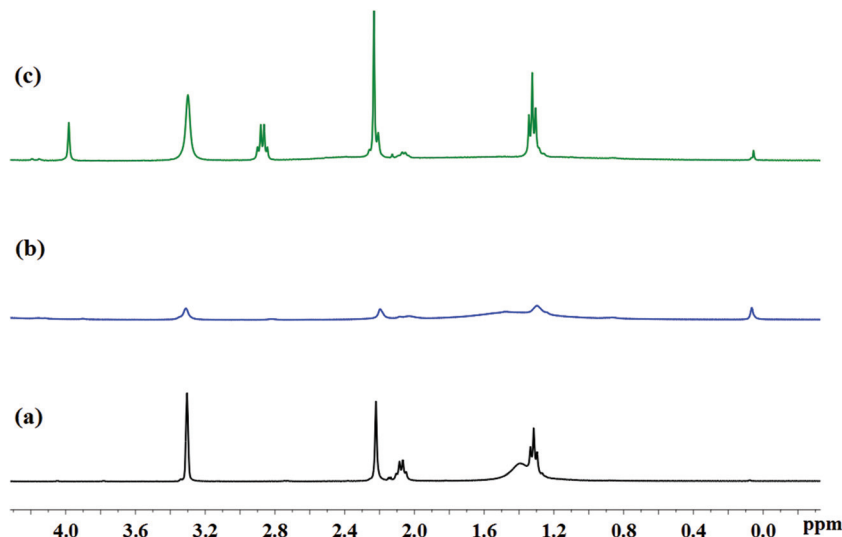


Fig. 6 $^1\text{H-NMR}$ spectra of complex **1** (a), after purging one (b) and two (c) NO equivalents in complex **1** in CD_3OD .

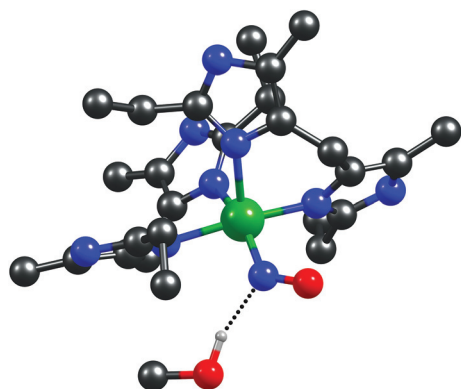


Fig. 7 The optimized structure, corresponding to the proposed intermediate; the color scheme is as follows: nickel: green, carbon: black, oxygen: red, nitrogen: blue and hydrogen: white; only the methanol hydrogen is shown in the structure. The rest of the hydrogen atoms were removed for clarity.

$150\text{--}200\text{ cm}^{-1}$, as has been observed in previous reports.^{43–46} Therefore, the value can be deemed to be acceptable.

In this regard, it is also noted that several other possible structures for the intermediate have been looked into computationally. This includes octahedral complexes having chlorine coordinated to the nickel centre, square planar complexes where one of the ligands is mono coordinated, and a trigonal geometry where both the ligands are mono coordinated. These possible structures are shown in the ESI.† It was found that none of the other structures were (a) able to form stabilized optimized minima or (b) comparable in stability (*i.e.* they were found to be energetically less stable) to the proposed intermediate structure. This provides further indication of the validity of the proposed intermediate complex.

Furthermore, the UV-Visible spectrum for the intermediate $\{\text{NiNO}\}^{10}$ complex in methanol was calculated with TD-DFT

calculations at the PBE/TZVP level of theory, with solvent corrections included. The intermediate complex showed three absorption bands: (i) at 428 nm with oscillator strength of 0.0035, (ii) at 521 nm with oscillator strength of 0.0036 and at 580 nm with oscillator strength of 0.0055. Therefore, the calculations indicated that the strong absorption band is at 580 nm, which is in agreement with the experimentally observed λ_{max} of 578 nm (Fig. 2). Thus, the current computational investigations suggest that the intermediate formed is indeed the square based pyramidal geometry wherein the NO is coordinated to the Ni(I) center, with a methanol solvent molecule hydrogen bonded to the nitrosyl nitrogen, as shown in the optimized structure in Fig. 6.

In the presence of excess NO, the intensity of 578 nm band of $\{\text{NiNO}\}^{10}$ was found to decay, indicating decomposition of the intermediate (Fig. 2). This finally lead to formation of the corresponding Ni(II)-nitrito complex (**2**) and nitrous oxide (N_2O) (Scheme 1). The final nitrito complex, **2** was isolated and characterized by various spectroscopic techniques (Experimental section). It behaves as a 1:1 electrolyte in solution (Experimental section). The single crystal X-ray structure revealed that a Ni(II) centre is coordinated to two ligand moieties and a $(\eta^2\text{-O,O})$ -nitrito group (Fig. 8). The crystallographic data, selected bond distances and angles are listed in Tables 1–3, respectively.

The average Ni–N distances (2.078 \AA) were found to be longer compared that in complex **1**, perhaps because of a geometry difference. The average N–O distance of the coordinated nitrito group was 1.268 \AA and the Ni–O distance was 2.124 \AA .

N_2O formation in the reaction was confirmed by GC-mass spectral analysis of the head space gas of the reaction vessel (yield, $\sim 60\%$; ESI†). This was further confirmed by the FT-IR monitoring of the reaction mixture, which showed the appearance of a stretching frequency at 2230 cm^{-1} that was assignable to N_2O (Fig. 4). Recently, Hayton *et al.* reported the

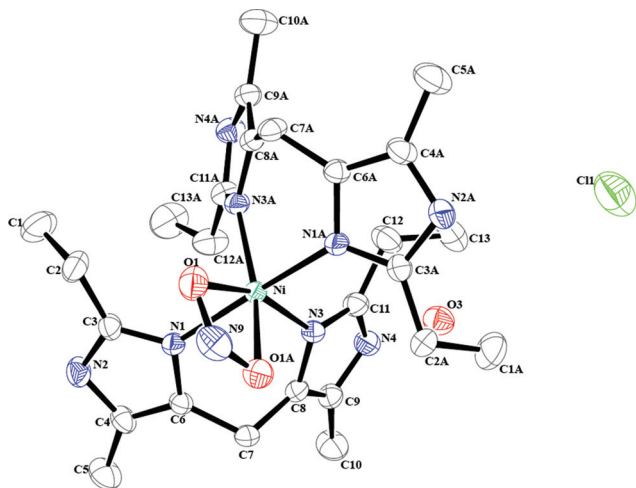


Fig. 8 ORTEP diagram of complex 2 (50% thermal ellipsoid plot, H-atoms are omitted for clarity).

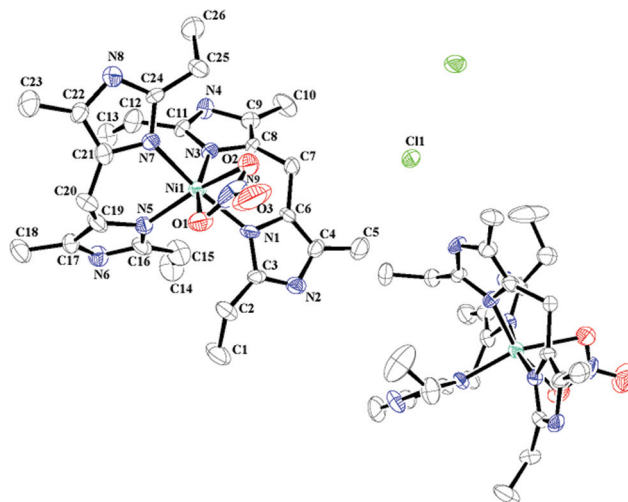


Fig. 9 ORTEP diagram of complex 3 (50% thermal ellipsoid plot, H-atoms omitted for clarity).

isolation of a nickel nitrosyl, $[\text{Ni}(\text{NO})(\text{bipy})_2](\text{PF}_6)_2$, which forms N_2O upon standing *via* a *cis*- $[\text{N}_2\text{O}_2]^{2-}$ intermediate. In this case, the N_2O stretching frequency appeared at 2228 cm^{-1} .^{29,30}

The formation of N_2O from NO can occur either by HNO disproportionation or by hyponitrite intermediate formation.⁴⁷ One proposed mechanism involves the initial formation of a *cis*-dinitrosyl complex followed by coupling of the two nitrosyl groups and subsequent reduction to form a hyponitrite, $(\text{N}_2\text{O}_2)^{2-}$ intermediate.^{47,48} Reaction with H^+ results in H_2O and N_2O . A solid state thermal decomposition study of various metal-nitrosyls reveals that the $[\text{M}(\text{NO})_2]$ motif actually plays an important role in the homogeneous solution phase reduction of NO to N_2O for various transition metal ions such as Rh , Ir , Ru , Fe and Pt .^{49,50}

On the other hand, the bent nitrosyl ligands are known to be the subject of electrophilic attack at the nitrogen lone pair.^{47,51} There are several examples reported on the electrophilic attack of free NO on a metal bound nitrosyl ligand.^{47,51} For instance, $[\text{Co}(\text{NO})(\text{NH}_3)_5]^{2+}$ is known to react with free NO to generate an asymmetric hyponitrite bridged dimer.^{51b} It has also been suggested that electrophilic attack of the free NO on that coordinated to the transition metal will result in a hyponitrite complex.⁴⁷ This decomposes to yield N_2O and water. The proposed mechanistic cycle of nitric oxide reductase activity of cytochrome *c* oxidase, it is believed that initial binding of NO to the reduced heme centre resulted in a bent nitrosyl (ν_{NO} , 1610 cm^{-1}).⁵² In subsequent steps, nitrogen–nitrogen bond formation was suggested through reaction of a second nitrosyl group bound to the copper centre of CcO .⁵²

It would be worth mentioning that mononuclear copper(i)-nitrosyl complexes were found to promote NO disproportionation with the $\text{Cu}(\text{ii})$ -nitrito complex formation.⁵³ For instance, $\text{Cu}(\text{i})$ complexes of bis-(phenyl) substituted tris-(pyrazole)-hydroborate and 1,4-diisopropyl-7,2-pyridylmethyl-1,4,7-triazacyclononane were reported to catalyze the disproportionation under an excess NO condition resulting in N_2O and corres-

ponding $\text{Cu}(\text{ii})(\text{NO}_2^-)$ complexes.⁵⁴ It can be noted that the X-ray crystallography characterization of the corresponding nitrito complexes revealed a symmetric $\eta^2\text{-O,O}$ -nitrite binding to the metal ions. Mechanistic studies suggested an electrophilic attack of a second NO molecule to the initially formed Cu-NO complex resulting in $\text{Cu}(\text{NO})_2$ species, which in subsequent N–N coupling and O-atom transfer obtains N_2O and a $\text{Cu}(\text{ii})$ ion nitrito complex.

The $\{\text{NiNO}\}^{10}$ intermediate was found to decompose to the corresponding nitrate complex (3) in the presence of oxygen (Scheme 1). Iron-nitrosyls in heme models and copper-nitrosyls are known to react with oxygen to afford peroxyntirite (ONOO^-), which then isomerises to the corresponding nitrate complexes.⁵⁵ The decomposition product, complex 3 was isolated as solid and characterized structurally. The solution conductance measurement suggested a 1 : 1 electrolytic nature of the complex. The perspective ORTEP view of complex 3 is shown in Fig. 9.

The single crystal X-ray structure suggests that the $\text{Ni}(\text{ii})$ centre is coordinated to two ligand moieties and a ($\eta^2\text{-O,O}$)-nitrate group (Fig. 9). The crystallographic data, selected bond distances and angles are listed in Tables 1–3, respectively. The average Ni–N distances (2.06 \AA) are shorter in comparison to complex 2 but longer with respect to complex 1. The average N–O distance of the coordinated nitrate group was 1.22 \AA and the Ni–O distance was 2.29 \AA .

Experimental section

Materials and methods

All reagents and solvents were purchased from commercial sources and were of reagent grade. HPLC grade methanol was used and dried using standard protocol. Deoxygenation of the solvent and solutions were affected by repeated vacuum and

purge cycles or bubbling with nitrogen or argon for 30 minutes. NO was used from a cylinder after purification by passing through KOH and P₂O₅ columns. Further purification was carried out following reported fractional distillation methods. A stoichiometric amount of NO was added to the sample using a Hamilton gas tight syringe after diluting with argon gas. The required NO dilution was affected with argon gas using an Environics Series 4040 computerized gas dilution system. UV-Visible spectra were obtained on an Agilent HP 8453 UV-Visible spectrophotometer. FT-IR spectra were obtained on a Perkin-Elmer spectrophotometer with either the sample prepared as KBr pellets or in solution in a potassium bromide cell. Solution electrical conductivity was checked using a Systronic 305 conductivity bridge. ¹H-NMR spectra were obtained with a 400 MHz Varian FT spectrometer. Chemical shifts (ppm) were referenced either with an internal standard (Me₄Si) for organic compounds or to the residual solvent peak. The X-band Electron Paramagnetic Resonance (EPR) spectra were obtained on a JES-FA200 ESR spectrometer at room temperature and 77 K with microwave power, 0.998 mW; microwave frequency, 9.14 GHz; and modulation amplitude, 2. The magnetic moment of the complexes were measured on a Cambridge magnetic balance. Mass spectra of the compounds were obtained in a Waters Q-ToF Premier and Aquity instrument. Elemental analyses were obtained with a Perkin Elmer Series II Analyzer.

Single crystals were grown by slow diffusion followed by a slow evaporation technique. The intensity data were collected using a Bruker SMART APEX-II CCD diffractometer, equipped with a fine focus 1.75 kW sealed tube MoK α radiation ($\lambda = 0.71073$ Å) at 273(3) K, with increasing ω (width of 0.3° per frame) at a 3 s per frame scan speed. The SMART software was used for data acquisition.⁵⁶ Data integration and reduction was undertaken with SAINT and XPREP software.⁵⁷ Structures were solved by direct methods using SHELXS-97 and refined with full-matrix least squares on F^2 using SHELXL-97.⁵⁸ Structural illustrations were drawn with ORTEP-3 for Windows.⁵⁹

Ligand L synthesis

2-Ethyl-4-methyl imidazole (2.2 g; 20 mmol) was taken in a round bottomed flask with 50 mL of methanol; to this 0.45 g of (15 mmol) formaldehyde and an aqueous 5.1 g (91 mmol) of potassium hydroxide solution was added dropwise. The reaction mixture was stirred for 24 h at room temperature. A white coloured solid was obtained. It was filtered off and washed with water. After washing the solid was dried in air and then placed in a desiccator overnight. Yield: 1.97 g (85%). Elemental analyses: Calcd (%) for C₁₃H₂₀N₄: C, 67.21; H, 8.68; N, 24.12. Found (%): C, 67.19; H, 8.68; N, 24.02. FT-IR (in KBr): 2964, 2842, 1614, 1529, 1455, 1071 cm⁻¹; ¹H-NMR (400 MHz, CDCl₃): δ_{ppm} , 3.53(2H), 2.44(4H), 1.87(6H), 1.08(6H). ¹³C-NMR (100 MHz, CDCl₃): δ_{ppm} , 149.2, 129.1, 127.2, 23.3, 22.6, 13.7, 10.6.

Complex 1 synthesis

Nickel(II) chloride hexahydrate (2.38 g) was taken in a 50 mL round bottomed flask and dissolved in 20 mL of MeOH. To

this, a solution of 4.64 g of ligand L in methanol (5 mL) was added and stirred for 1 h. The light green solution turned a deep green and after drying with a rotary evaporator and a green solid was obtained, which upon crystallization gave yellow crystals. Yield: 5.26 g (84%). CCDC no. 985705. Elemental analyses: Calcd For C₂₆H₄₀Cl₂N₈Ni: C, 52.55; H, 6.78; N, 18.86. Found (%): C, 52.61; H, 6.77; N, 18.95. FT-IR (in KBr): 3435, 2980, 1643, 1468, 1432, 1319, 1287, 1089, 816, 591 cm⁻¹. ¹H-NMR (400 MHz, CDCl₃): δ_{ppm} , 2.22(6H), 2.06(4H), 1.39(2H), 1.31(6H). ¹³C-NMR (100 MHz, CDCl₃): δ_{ppm} , 151.8, 131.2, 123.8, 23.7, 21.4, 13.5, 9.0. Molar conductance: 239 S cm² mol⁻¹ (in methanol).

Complex 2

In 20 mL of dry and degassed methanol solution of complex 1 (180 mg), freshly prepared nitric oxide was bubbled in excess until the deep colour of the solution faded. The reaction mixture was placed at room temperature for crystallization. Yield: 138.5 mg (72%). CCDC no. 1456771. Elemental analyses: Calcd For C₂₆H₄₀ClN₉O₄Ni: C, 49.04; H, 6.33; N, 19.79. Found (%): C, 49.11; H, 6.36; N, 19.92. FT-IR (in KBr): 3390, 3174, 3126, 1627, 1530, 1464, 1429, 1322, 1197, 1048, 776 cm⁻¹. UV: $\lambda(\epsilon/\text{mol}^{-1} \text{cm}^{-1})$, 621 (32), 979 (14). Molar conductance: 160 S cm² mol⁻¹ (in methanol), observed magnetic moment: 1.93 BM.

Complex 3

To a degassed methanol solution of complex 1 (240 mg) at -80 °C, freshly prepared nitric oxide was bubbled through for 30 s. Then, the excess NO gas was removed using four cycles of vacuum and Ar purging. To this, an excess of dioxygen was added through a gas tight syringe. The reaction mixture was warmed up to room temperature and kept for two days while complex 3 crystallized out. Yield: 128 mg (~52%). CCDC no. 1456772. Elemental analyses: Calcd For C₂₆H₄₀ClN₉O₅Ni: C, 47.84; H, 6.17; N, 19.31. Found (%): C, 47.91; H, 6.16; N, 19.40. FT-IR (in KBr): 3168, 3127, 3126, 1625, 1531, 1464, 1429, 1384, 1333, 1222, 1053, 839, 752, 620 cm⁻¹. UV: $\lambda(\epsilon/\text{mol}^{-1} \text{cm}^{-1})$, 600 (41), 987 (11). Molar conductance: 176 S cm² mol⁻¹ (in methanol), observed magnetic moment: 1.84 BM.

In situ generation of Ni(I) and Ni(I)-NO intermediates

Complex 1 (200 mg) was dissolved in 20 ml of dry methanol in a 50 mL Schlenk flask and then the solution was degassed with bubbling argon for 1 h. The solution was then cooled to -80 °C and an equivalent amount of nitric oxide gas was purged into the solution using a gas tight Hamilton syringe. The color of the solution became light, indicating formation of a Ni(I) intermediate. The reaction mixture was transferred into EPR and NMR tubes using a gas tight Hamilton syringe and the spectra were obtained.

A similar procedure was followed to generate {NiNO}¹⁰ wherein two NO equivalents were added resulting in a blue solution.

Conclusion

In conclusion, the Ni(II) complex of bis(2-ethyl-4-methylimidazol-5-yl)methane, **1** in methanol solution reacted with NO to result in reductive nitrosylation forming a corresponding {NiNO}¹⁰ intermediate. This intermediate upon subsequent reaction with an additional NO resulted in the release of N₂O and Ni(II)-nitrito complex formation. The crystallographic characterization of the nitrito complex revealed a symmetric η²-O,O-nitrito bonding to the metal ion as observed in cases of iron, manganese and copper complexes.

Acknowledgements

BM would like to thank Department of Science and Technology, India for financial support (SR/S1/IC-38/2010); DST-FIST for the X-ray diffraction facility. SG gratefully acknowledges IIT Guwahati for providing a research fellowship.

References

- (a) *Nitric Oxide: Biology and Pathobiology*, ed. L. J. Ignarro, Academic Press, San Diego, CA, 2000; (b) C. T. Martin, R. H. Morse, R. M. Kanne, H. B. Gray, B. G. Malmstrom and S. I. Chan, *Biochemistry*, 1981, **20**, 5147.
- (a) C. E. Cooper, J. Torres, M. A. Sharpe and M. T. Wilson, *FEBS Lett.*, 1997, **414**, 281; (b) G. B. Richter-Addo and P. Legzdins, *Metal Nitrosyls*, Oxford University Press, New York, 1992; (c) G. Studbauer, P. Giuffre and P. Sarti, *J. Biol. Chem.*, 1999, **274**, 28128; (d) J. A. McCleverty, *Chem. Rev.*, 2004, **104**, 403; (e) Y. Arikawa and M. Onishi, *Coord. Chem. Rev.*, 2012, **256**, 468.
- (a) A. K. Patra, M. J. Rose, M. M. Olmstead and P. K. Mascharak, *J. Am. Chem. Soc.*, 2004, **126**, 4780; (b) A. K. Patra, R. K. Afshar, J. M. Rowland, M. M. Olmstead and P. K. Mascharak, *Angew. Chem., Int. Ed.*, 2003, **42**, 4517; (c) A. K. Patra, J. M. Rowland, D. S. Marlin, E. Bill, M. M. Olmstead and P. K. Mascharak, *Inorg. Chem.*, 2003, **42**, 6812.
- (a) J. C. W. Chien, *J. Am. Chem. Soc.*, 1969, **91**, 2166; (b) B. B. Wayland and L. W. Olson, *J. Am. Chem. Soc.*, 1974, **96**, 6037.
- (a) M. Hoshino, M. Maeda, R. Konishi, H. Seki and P. C. Ford, *J. Am. Chem. Soc.*, 1996, **118**, 5702; (b) M. Hoshino, K. Ozawa, H. Seki and P. C. Ford, *J. Am. Chem. Soc.*, 1993, **115**, 9568; (c) N. Lehnert, V. K. K. Praneeth and F. Paulat, *J. Comput. Chem.*, 2006, **27**, 1338.
- (a) B. O. Fernandez and P. C. Ford, *J. Am. Chem. Soc.*, 2003, **125**, 10510; (b) B. O. Fernandez, I. M. Lorkovic and P. C. Ford, *Inorg. Chem.*, 2004, **43**, 5393.
- (a) M. K. Ellison and W. R. Scheidt, *J. Am. Chem. Soc.*, 1999, **121**, 5210; (b) D. P. Linder, K. R. Rodgers, J. Banister, G. R. A. Wyllie, M. K. Ellison and W. R. Scheidt, *J. Am. Chem. Soc.*, 2004, **126**, 14136.
- (a) M. D. Lim, I. M. Lorkovic and P. C. Ford, *J. Inorg. Biochem.*, 2005, **99**, 151; (b) D. Shamir, I. Zilbermann, E. Maimon, G. Gellerman, H. Cohen and D. Meyerstein, *Eur. J. Inorg. Chem.*, 2007, 5029.
- A. C. F. Gorren, E. de Boer and R. Wever, *Biochim. Biophys. Acta*, 1987, **916**, 38.
- J. Torres, C. E. Cooper and M. T. Wilson, *J. Biol. Chem.*, 1998, **273**, 8756.
- (a) J. Torres, D. Svistunenko, B. Karlsson, C. E. Cooper and M. T. Wilson, *J. Am. Chem. Soc.*, 2002, **124**, 963; (b) G. C. Brown, *Biochim. Biophys. Acta*, 2001, **1504**, 46.
- (a) J. Torres, M. A. Sharpe, A. Rosquist, C. E. Cooper and M. T. Wilson, *FEBS Lett.*, 2000, **475**, 263; (b) H. J. Wijma, G. W. Canters, S. de Vries and M. P. Verbeet, *Biochem.*, 2004, **43**, 10467.
- K. M. Miranda, X. Bu, I. M. Lorkovic and P. C. Ford, *Inorg. Chem.*, 1997, **36**, 4838.
- (a) I. M. Lorkovic, K. M. Miranda, B. Lee, S. Bernhard, J. R. Schoonover and P. C. Ford, *J. Am. Chem. Soc.*, 1998, **120**, 11674; (b) I. M. Lorkovic and P. C. Ford, *Inorg. Chem.*, 1999, **38**, 1467.
- (a) I. M. Lorkovic and P. C. Ford, *J. Am. Chem. Soc.*, 2000, **122**, 6516; (b) L. E. Laverman, A. Wanat, J. Oszajca, G. Stochel, P. C. Ford and R. van Eldik, *J. Am. Chem. Soc.*, 2001, **123**, 285.
- (a) L. E. Laverman and P. C. Ford, *J. Am. Chem. Soc.*, 2001, **123**, 11614; (b) T. S. Kurtikyan, G. G. Martirosyan, I. M. Lorkovic and P. C. Ford, *J. Am. Chem. Soc.*, 2002, **124**, 10124.
- (a) M. D. Lim, I. M. Lorkovic, K. Wedeking, A. W. Zanella, C. F. Works, S. M. Massick and P. C. Ford, *J. Am. Chem. Soc.*, 2002, **124**, 9737; (b) J. C. Patterson, I. M. Lorkovic and P. C. Ford, *Inorg. Chem.*, 2003, **42**, 4902.
- (a) P. C. Ford, *Pure Appl. Chem.*, 2004, **76**, 335; (b) G. G. Martirosyan, A. S. Azizyan, T. S. Kurtikyan and P. C. Ford, *Chem. Commun.*, 2004, 1488.
- (a) T. S. Kurtikyan, G. M. Gulyan, G. G. Martirosyan, M. D. Lim and P. C. Ford, *J. Am. Chem. Soc.*, 2005, **127**, 6216; (b) P. C. Ford, B. O. Fernandez and M. D. Lim, *Chem. Rev.*, 2005, **105**, 2439.
- (a) A. J. Gow, B. P. Luchsinger, J. R. Pawloski, D. J. Singel and J. S. Stamler, *Proc. Natl. Acad. Sci. U. S. A.*, 1999, **96**, 9027; (b) B. P. Luchsinger, E. N. Rich, A. J. Gow, E. M. Williams, J. S. Stamler and D. J. Singel, *Proc. Natl. Acad. Sci. U. S. A.*, 2003, **100**, 461.
- (a) M. T. Gladwin, J. R. Lancaster Jr., B. A. Freeman and A. N. Schechter, *Nat. Med.*, 2003, **9**, 496; (b) T. H. Han, J. M. Fukuto and J. C. Liao, *NO Bio. Chem.*, 2004, **10**, 74.
- (a) M. S. Feelisch, T. Rassaf, S. Manimneh, N. Singh, N. S. Bryan, D. Jour'd'Heuil and M. Kelm, *FASEB J.*, 2002, **16**, 1775; (b) N. S. Bryan, T. Rassaf, R. E. Maloney, C. M. Rodriguez, F. Saijo, J. R. Rodriguez and M. Feelisch, *Proc. Natl. Acad. Sci. U. S. A.*, 2004, **101**, 4308.

- 23 (a) T. Rassaf, M. Feelisch and M. Kelm, *Free Radicals Biol. Med.*, 2004, **36**, 413; (b) N. S. Bryan, B. O. Fernandez, S. M. Bauer, M. F. Garcia-Saura, A. B. Milsom, T. Rassaf, R. E. Maloney, A. Bharti, J. Rodriguez and M. Feelisch, *Nat. Chem. Biol.*, 2005, **1**, 290.
- 24 A. A. Eroy-Reveles, Y. Leung, C. M. Beavers, M. M. Olmstead and P. K. Mascharak, *J. Am. Chem. Soc.*, 2008, **130**, 4447.
- 25 K. Ghosh, A. A. Eroy-Reveles, M. M. Olmstead and P. K. Mascharak, *Inorg. Chem.*, 2005, **44**, 8469.
- 26 (a) M. A. Halcrow and G. Christou, *Chem. Rev.*, 1994, **94**, 2421; (b) L. Signor, C. Knuppe, R. Hug, B. Schweizer, A. Pfaltz and B. Jaun, *Chem. – Eur. J.*, 2000, **6**, 3508.
- 27 (a) S. Ozaki, H. Matsushita and H. Ohmori, *J. Chem. Soc., Perkin Trans. 1*, 1993, 649; (b) C. J. Campbell, J. F. Rusling and C. Brückner, *J. Am. Chem. Soc.*, 2000, **122**, 6679.
- 28 (a) S. V. Kryatov, B. S. Mohanraj, V. V. Tarasov, O. P. Kryatova, E. V. Rybak-Akimova, B. Nuthakki, J. F. Rusling, R. J. Staples and A. Y. Nazarenko, *Inorg. Chem.*, 2002, **41**, 923; (b) T. L. James, L. Cai, M. C. Muetterties and R. H. Holm, *Inorg. Chem.*, 1996, **35**, 4148.
- 29 (a) A. M. Wright, G. Wu and T. W. Hayton, *J. Am. Chem. Soc.*, 2012, **134**, 9930; (b) A. M. Wright, H. T. Zaman, G. Wu and T. W. Hayton, *Inorg. Chem.*, 2014, **53**, 3108.
- 30 (a) A. M. Wright, H. T. Zaman, G. Wu and T. W. Hayton, *Inorg. Chem.*, 2013, **52**, 3207; (b) A. M. Wright, G. Wu and T. W. Hayton, *Inorg. Chem.*, 2011, **50**, 11746.
- 31 A. Kalita, P. Kumar, R. C. Deka and B. Mondal, *Chem. Commun.*, 2012, **48**, 1551.
- 32 (a) R. J. Butcher and E. Sinn, *Inorg. Chem.*, 1977, **16**, 2334; (b) H. Ohtsu and K. Tanaka, *Inorg. Chem.*, 2004, **43**, 3024.
- 33 (a) S. V. Kryatov, B. S. Mohanraj, V. V. Tarasov, O. P. Kryatova, E. V. Rybak-Akimova, B. Nuthakki, J. F. Rusling, R. J. Staples and A. Y. Nazarenko, *Inorg. Chem.*, 2002, **41**, 923; (b) B. J. Hathaway and D. E. Billing, *Coord. Chem. Rev.*, 1970, **5**, 143; (c) R. R. Gagne and D. M. Ingle, *Inorg. Chem.*, 1981, **20**, 420; (d) K. Nag and A. Chakravorty, *Coord. Chem. Rev.*, 1980, **33**, 87; (e) C. W. G. Ansell, J. Lewis, P. R. Raithby, J. N. Ramsden and M. Schröder, *J. Chem. Soc., Chem. Commun.*, 1982, 546; (f) M. P. Suh, K. Y. Oh, J. W. Lee and Y. Y. Bae, *J. Am. Chem. Soc.*, 1996, **118**, 777.
- 34 R. D. Feltham and J. T. Carriel, *Inorg. Chem.*, 1964, **3**, 121.
- 35 (a) V. K. Landry and G. Parkin, *Polyhedron*, 2007, **26**, 4751; (b) Z. A. Del, A. Mezzetti, V. Novelli, P. Rigo, M. Lanfranchi and A. Tiripicchio, *Dalton Trans.*, 1990, 1035; (c) B. C. Fullmer, M. Pink, H. Fan, X. Yang, M.-H. Baik and K. G. Caulton, *Inorg. Chem.*, 2008, **47**, 3888; (d) A. G. Tennyson, S. Dhar and S. J. Lippard, *J. Am. Chem. Soc.*, 2008, **130**, 15087; (e) M. S. Varonka and T. H. Warren, *Organometallics*, 2010, **29**, 717.
- 36 P. Legzdins and G. B. Richter-Addo, *Metal Nitrosyls*, Oxford University Press, New York, 1992.
- 37 R. Ahlrichs, M. Baer, M. Haeser, H. Horn and C. Koelmel, *Chem. Phys. Lett.*, 1989, **162**, 165.
- 38 J. P. Perdew, K. Burke and M. Ernzerhof, *Phys. Rev. Lett.*, 1996, **77**, 3865.
- 39 F. Weigend, *Phys. Chem. Chem. Phys.*, 2002, **4**, 4285.
- 40 K. Eichkorn, O. Treutler, H. Oehm, M. Haeser and R. Ahlrichs, *Chem. Phys. Lett.*, 1995, **240**, 283.
- 41 M. Sierka, A. Hogekamp and R. Ahlrichs, *J. Chem. Phys.*, 2003, **118**, 9136.
- 42 A. Klamt, *J. Phys. Chem.*, 1995, **99**, 2224.
- 43 N. Sundaraganesan, S. Kalaichelvan, C. Meganathan, B. D. Joshua and J. Cornard, *Spectrochim. Acta, Part A*, 2008, **71**, 898.
- 44 M. Karabacak and M. Kurt, *Spectrochim. Acta, Part A*, 2008, **71**, 876.
- 45 M. Karabacak, D. Karagaz and M. Kurt, *J. Mol. Struct.*, 2008, **892**, 25.
- 46 L. Fan and T. Ziegler, *J. Chem. Phys.*, 1992, **96**, 9005.
- 47 J. H. MacNeil, P. A. Berseth, E. L. Bruner, T. L. Perkins, Y. Wadia, G. Westwood and W. C. Trogler, *J. Am. Chem. Soc.*, 1997, **119**, 1668.
- 48 R. Eisenberg and D. E. Hendricksen, *Adv. Catal.*, 1979, **28**, 79.
- 49 (a) D. E. Hendricksen, C. D. Meyer and R. Eisenberg, *Inorg. Chem.*, 1977, **16**, 970; (b) B. L. Haymore and J. A. Ibers, *J. Am. Chem. Soc.*, 1974, **96**, 3325.
- 50 (a) K. A. Pearsall and F. T. Bonner, *Inorg. Chem.*, 1982, **21**, 1978; (b) S. Bhaduri, B. F. G. Johnson, C. J. Savory, J. A. Segal and R. H. Walter, *J. Chem. Soc., Chem. Commun.*, 1974, 809.
- 51 (a) D. Gwost and K. G. Caulton, *Inorg. Chem.*, 1974, **13**, 414; (b) B. F. Hoskins, F. D. Whillans, D. H. Dale and D. C. Hodgkin, *J. Chem. Soc., Chem. Commun.*, 1969, **69**.
- 52 (a) X.-J. Zhao, V. Sampath and W. S. Caughey, *Biochem. Biophys. Res. Commun.*, 1994, **204**, 537; (b) G. W. Brudwig, T. H. Stevens and S. I. Chan, *Biochemistry*, 1980, **19**, 5275.
- 53 (a) J. L. Schneider, S. M. Carrier, C. E. Ruggiero, J. V. E. Young and W. B. Tolman, *J. Am. Chem. Soc.*, 1998, **120**, 11408.
- 54 C. E. Ruggiero, S. M. Carrier, W. E. Antholine, J. W. Whittaker, C. J. Cramer and W. B. Tolman, *J. Am. Chem. Soc.*, 1993, **115**, 11285.
- 55 (a) G. A. Park, S. Deepalatha, S. C. Puiu, D.-H. Lee, B. Mondal, A. A. N. Sarjeant, D. del Rio, M. Y. M. Pau, E. D. Solomon and K. D. Karlin, *J. Biol. Inorg. Chem.*, 2009, **14**, 1301; (b) S. Goldstein, J. Lind and G. Merenyi, *Chem. Rev.*, 2005, **105**, 2457; (c) S. Herold and W. H. Koppenol, *Coord. Chem. Rev.*, 2005, **249**, 499 and reference therein.
- 56 *SMART, SAINT and XPREP*, Siemens Analytical X-ray Instruments Inc., Madison, Wisconsin, USA, 1995.
- 57 G. M. Sheldrick, *SADABS: Software for Empirical Absorption Correction*, University of Gottingen, Institut für Anorganische Chemie der Universität, Tammanstrasse 4, D-3400 Gottingen, Germany, 1999–2003.
- 58 G. M. Sheldrick, *SHELXS-97*, University of Gottingen, Germany, 1997.
- 59 L. J. Farrugia, *J. Appl. Crystallogr.*, 1997, **30**, 565.